NOVA SCHOOL OF SCIENCE & TECHNOLOGY

DEPARTMENT OF PHYSICS

CARLOTA SOARES SANTOS CAMARATE

DEVELOPING OF A MONTE CARLO MODEL TO ESTIMATE THE RADIOSENSITIZER EFFECTS OF METALLACARBORANES IN TUMOUR CELLS

MASTER IN PHYSICS ENGINEERING

NOVA University Lisbon

April 2, 2024

NOVA SCHOOL OF SCIENCE & TECHNOLOGY

DEPARTAMENT OF PHYSICS

DEVELOPING OF A MONTE CARLO MODEL TO ESTIMATE THE RADIOSENSITIZER EFFECT OF METALLACARBORANES IN TUMOUR CELLS

CARLOTA SOARES SANTOS CAMARATE

Advisers: João Duarte Neves Cruz
Associate Professor, NOVA University Lisbon
Salvatore Di Maria
Guest Assistant Professor, University of Lisbon

Examination Committee:

Chair: Name of the committee chairperson,
Full Professor, FCT-NOVA

Rapporteurs: Name of a rapporteur,
Associate Professor, Another University
Name of another rapporteur,
Assistant Professor, Another University

Adviser: Name of the adviser present in defence,
Associate Professor, University

Members: Yet another member of the committee,
Full Professor, Another University
Yet another member of the committee,
Assistant Professor, Another University

MASTER'S IN PHYSICS ENGENEERING

NOVA University Lisbon
April, 2024

Developing of a Monte Carlo model to estimate the radiosensitizer effect of metallacarboranes in tumour cells

ACKNOWLEDGMENTS

Because no work is ever achieved by one alone, here are my acknowledgements to all those who helped and supported me throughout the course of this work.

Em primeiro lugar e mais importante, aos meus orientadores, Doutor Salvatore di Maria e Doutor João Cruz, por todo o apoio e dedicação, por me terem incentivado sempre a continuar mesmo quando os obstáculos apareciam e por nunca terem desistido de mim. A toda a restante equipa que conheci no CTN, Doutor Luís Alves, Doutora Teresa Pinheiro, Doutora Ana Belchior e Doutora Fernanda Marques, o meu enorme obrigada por todo o apoio, por estarem sempre disponíveis para me ensinar e sempre prontos a discutir resultados, este trabalho não teria sido concluído sem o vosso apoio.

Aos meus coordenadores de curso ao longo dos anos, Doutora Isabel Catarino, Doutor André Wemans e Doutor Paulo Ribeiro, por estarem sempre disponíveis para qualquer questão, por todas as exceções abertas ao longo dos anos, todos os emails respondidos a qualquer hora e todos os requerimentos aceites, o meu muito obrigada.

Aos meus brownies, os amigos que fazemos na faculdade e que se tornam mais que isso, obrigada por me acompanharem ao longo desta fase tão marcante nas nossas vidas. Às minhas queridas gémeas, apesar do nosso percurso ter seguido caminhos diferentes, obrigada por estarem lá sempre para me ouvir falar de física, mesmo quando não entendiam nada.

Aos meus pontinhos, membros do Ponto Zero, e em especial aos meus treinadores, João e Pascoal, obrigada por serem a minha família fora de casa, por serem uma fonte de dopamina e por compreenderem sempre quando precisava de faltar para estudar e serem sempre os primeiros a apoiar-me.

Por fim, à minha família: sim, já entreguei a tese.

"Do or do not. There is no try."
(Yoda).

ABSTRACT

Despite technological and medical evolution, cancer is still one of the leading causes of death worldwide, having accounted for almost one in every six deaths in 2020. Radiotherapy is one of the treatments possible for cancer and, in particular, radiotherapy using protons has been more explored by scientists and researchers in the latest decades, because of its higher linear energy transmit (LET) and localized absorbed dose delivering to tumour target cells, limiting the damages caused in surrounding healthy tissues. The use of radiosensitizers to increase the local absorbed dose in the tumour cells during irradiation is a modality that has also been explored in the recent years, since it could potentially increase the efficacy of the radiation treatment.

In this context, this work aims to verify the effectiveness of using metallacarboranes as radiosensitizers in proton therapy, mainly by studying the occurrence of the proton-boron fusion reaction, able to produce alpha particles, which, given their energy and small penetration depth, could be very effective in killing tumour cells.

In order to accomplish this objective, both experimental and simulation studies were performed. Monte Carlo (MC) simulation program, TOPAS, was used to model the irradiation conditions (e.g., proton flux, energy distribution) of the microprobe from the Van de Graaff accelerator in the laboratory of Campus Tecnológico e Nuclear, IST, Universidade de Lisboa. In addition, from the radiobiological point of view, experimental irradiations were performed for samples of cells with and without a metallacarborane, COSANE, in order to calculate the cell survival rate. The MC model here developed permitted to perform several dose assessments for the experimental setup used in this work. In agreement with other literature studies, for the ^{11}B concentration used in this work, MC dose results, considering the effects of also alpha particles, confirmed no radio sensitizing effect due to the presence of boron. Additional experimental work will be necessary to better understand the role of ^{11}B in eventual p-^{11}B treatments.

The research work described in this dissertation was carried out in accordance with the norms established in the ethics code of Universidade Nova de Lisboa. The work described and the material presented in this dissertation, with the exceptions clearly indicated, constitute original work carried out by the author.

RESUMO

Apesar da evolução tecnológica e médica, o cancro ainda é uma das principais causas de morte a nível mundial, tendo sido responsável por quase uma em cada seis mortes em 2020. A radioterapia é um dos tratamentos possíveis para o cancro e, em particular, a radioterapia com recurso a protões tem sido mais explorada por cientistas e investigadores nas últimas décadas, devido à sua maior transmissão linear de energia (LET) e dose absorvida localizada nas células alvo do tumor, limitando os danos causados nos tecidos saudáveis circundantes. O uso de radiossensibilizadores para aumentar a dose absorvida nas células tumorais durante a irradiação é uma modalidade que também tem vindo a ser explorada nos últimos anos, pois pode aumentar potencialmente a eficácia da radioterapia.

Neste contexto, este trabalho tem como objetivo verificar a eficácia da utilização de metalacarboranos como radiosensibilizador na terapia de protões, principalmente através do estudo da ocorrência da reação de fusão protão-boro, que produz de partículas alfa, que, dada a sua energia e pequeno alcance, podem ser muito eficazes a matar células tumorais.

Para atingir este objetivo, foram realizados estudos experimentais e de simulação. O programa de simulação Monte Carlo (MC), TOPAS, foi utilizado para modelar as condições de irradiação (por exemplo, fluxo de protões, distribuição de energia) da microssonda do acelerador Van de Graaff no laboratório do Campus Tecnológico e Nuclear, IST, Universidade de Lisboa. Além disso, do ponto de vista radiobiológico, foram realizadas irradiações experimentais em amostras de células com e sem COSANE, para calcular a taxa de sobrevivência celular. O modelo MC aqui desenvolvido permitiu realizar diversas avaliações de dose para a configuração experimental utilizada neste trabalho. De acordo com outros estudos da literatura, para a concentração de ^{11}B utilizada neste trabalho, os resultados da dose de MC, considerando os efeitos também das partículas alfa, não confirmam nenhum efeito radiosensibilizador devido à presença de boro. Será necessário um trabalho experimental adicional para compreender melhor o papel do ^{11}B em eventuais tratamentos com p-^{11}B.

O trabalho de investigação descrito nesta dissertação foi realizado de acordo com as normas estabelecidas no código de ética da Universidade Nova de Lisboa. O trabalho descrito e o material apresentado nesta dissertação, com as exceções claramente indicadas, constituem trabalho original realizado pela autora.

CONTENTS

LIST OF FIGURES

LIST OF TABLES

ACRONYMS

BNCT – Boron Neutron Capture Therapy
PBF(T) – Proton Boron Fusion (Therapy)
LET – Linear Energy Transfer
TOPAS – TOol for PArticle Simulation
PDG – Particle Data Group
PIXE – Particle Induced X-ray Emission
RBS – Rutherford Backscattering Spectrometry
DMEM – Dulbecco's Modified Eagle's Medium
UV – Ultraviolet
PBS – Phosphate Buffered Saline
NIST - National Institute of Standards and Technology

1

INTRODUCTION

Trachea, bronchus and lung cancers were the sixth leading cause of death in the world in 2019 [1]. Despite the decrease of overall deaths by cancer observed since 2000, it is still a very prominent cause; according to the World Health Organization's most recent statistics [2], cancer in 2020 accounted for nearly 10 million deaths, which is equivalent to almost one out of every six deaths worldwide.

Currently, the possible treatments available for cancer are surgery, radiotherapy and systemic therapy, this last one being treatments that affect the entire body such as chemotherapy and hormonal treatments.

Radiotherapy can be performed using several types of radiation, with X-ray treatments still being the most commonly used [3]. However, since it started being used in the seventies [4], proton therapy has shown to have benefits in comparison to X-rays, mainly considering protons can better target the tumours, causing less damage in surrounding healthy tissues. There are still many studies being conducted on this form of therapy to verify its advantages in comparison to other more used radiations [5].

Another particle that raises interest in the area of radiotherapy is the alpha particle. Alpha particles have a high LET (greater than 100 $keV \cdot \mu m^{-1}$) and low range in tissue (tens of micrometres) [5]. This makes these particles ideal for radiation therapy, as they give a high local dose to tumour cells without damaging the surrounding ones. As an example, in Boron Neutron Capture Therapy (BNCT) when atoms of ^{10}B are irradiated by thermal neutrons (energy <0.1 eV), ^{10}B becomes a ^{11}B and then disintegrates into an alpha particle and a ^{7}Li, with average kinetic energy of 2.33 MeV. It is also relevant this reaction's unusually large thermal neutron capture cross-section [6]. This therapy is now an already accepted method of treatment [7]. Nonetheless, when considering boron isotopes' natural abundance (^{10}B), they account for only 19.9%, while ^{11}B accounts for 80.1%. In addition, in BNCT neutrons represent some drawback related to the damage of normal tissue following neutron irradiation [7] .

With the interest that arose in the use of proton beams for therapy and the studies on the Proton Boron Fusion (PBF) reaction that permits the release of three alpha particles instead of just one [8], a Proton Boron Fusion Therapy (PBFT) rises as a possible more effective alternative to the current existing radiotherapies.

With this work, the goal was to simulate the irradiation of cells with metallacarboranes to verify the dose augmentation when compared to cells without these compounds, resorting to a Monte Carlo simulation program, TOPAS, while in parallel irradiate culture tumour cells with the compound to compare the results obtained through simulation and in experiments.

2

STATE OF THE ART

In this chapter, I will introduce an overview of what already exists in terms of radiotherapy using boron, as well as a more detailed view on the $^{11}B(p,\alpha)\alpha\alpha$ reaction and its importance in proton radiotherapy and the possible applications of metallacarboranes, particularly in medical treatments.

$^{11}B(p, \alpha)\alpha\alpha$ Reaction

The relevance of this reaction comes from the interest that arose in the use of protons in radiotherapy, due to the properties of charged particles, that are capable of depositing energy much more selectively than other particles, as represented by the Bragg peak that describes the inverse relation between dose and depth, which indicates that healthy tissues are spared of high doses, while the maximum dose is confined to the area surrounding the particle beam's maximum reach [9].

The nuclear fusion reaction $^{11}B(p, \alpha)\alpha\alpha$ can be described as a reaction composed by two parts: first, the interaction of a proton with the boron atom leads to the occurrence of a fusion reaction, originating a carbon atom (^{12}C) in an excited state. This carbon atom then separates in an alpha particle and a beryllium atom (^{8}Be). The decay of the carbon atom into an alpha particle and a beryllium atom depends in which excited state the carbon is: if the carbon is in the excited state 2-, it decays to the 2+ state of the ^{8}Be, emitting an alpha particle with l^1=3; if it is the excited state 3-, the resulting alpha particle can have l=1 or l=3, according to whether the beryllium atom emitted in the decay is in the excited state 2+ or in the fundamental state 0+. Independent of the state the beryllium is, it quickly also separates into two alpha particles with l=2, which present an isotropic, well-defined energy distribution[9][10]. This reaction has a resonance at 675keV with a cross section of 0.9 barn [11].

[1] Orbital angular momentum

Metallacarboranes

Metallacarboranes are an example of radiosensitizers. Radiosensitizers are agents that make tumour cells more sensitive to radiotherapy. The first combination of the use of a chemical compound and radiotherapy can be dated to more than 100 years ago [12]. Some commonly used radiosensitizers are cisplatin and gemcitabine [13], but with the advances of nanotechnology, nanoparticles are surging as new form of cancer treatment, due to their higher biocompatibility, tumour targeting and stability (when compared to conventionally used drugs) [14].

The metallacarboranes originated around the sixties when polyhedral borane chemistry and transition metal organometallics were combined. These present a vast range of possible applications, including medical ones [15].

The carboranes are molecules that contain at least one atom of carbon with a delocalized electron bound. In turn, the metallacarboranes are carboranes that have at least one metal atom. The bond with the delocalized electron makes these compounds more stable, minimizing the oxidation and reduction effects, making them robust and managed in common solvents [15]. The carboranes present the capacity of adding tri dimensional substituents in opposition to organic based compounds, which do it bidimensionally, making these compounds more adaptable. The metallacarboranes share this versability presented by the carboranes, adding some metallic properties and presenting thermic and chemical stability [16].

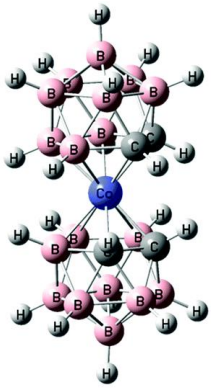

$H[Co(C_2B_9H_{11})_2]$
H[COSANE]

Figure 1 - COSANE molecule

Metallacarboranes combine an organic polymeric matrix with an inorganic filler [17] and have a chemical formula $[M(C_2B_9H_{11})_2]$, where M is a metal, typically Fe or Co. This central metal is the common vertex of two joined by one vertex icosahedron. These molecules are small with a cylindrical shape (0.6 nm x 1.1 nm) and are also water-soluble [18].

For this project, COSANE was the metallacarborane chosen because of the Boron atoms it has, since the main focus was to study the boron proton fusion reaction.

3

MATERIALS AND METHODS

In this chapter I will introduce what is a Monte Carlo Model, in particular the TOPAS simulation software, which was the tool used in this work, explaining its operation method and detailing the simulation setup created as well. I will also introduce the experimental setup, with focus on the accelerator used, and the methods used to prepare, irradiate and analyse cells. To note, this worked began by performing theoretical calculations (that can be found in RESULTS) to confirm the protons reached 675 keV within the cell, then the experimental work was done and only after did the simulation work began, therefore why many things were tested without the use of simulations.

Monte Carlo Model

The goal of a Monte Carlo model is to create an independent set of random data, through the generation of pseudorandom numbers, using probability laws [19]. It aims to solve purely deterministic problems, using random samples of certain probabilistic distributions. It presents an extensive number of applications and is very used due to its simplicity, keeping efficiency and rigor [20].

The most typical uses of these models can be divided in sampling, estimation and optimization. The sampling has as purpose to collect information about a random event through multiple times observation [20]. This was the intended use of the model in this work, since the irradiation of boron with a proton beam was simulated multiple times, in order to study the occurrence of the reaction $^{11}B(p, \alpha)\alpha\alpha$.

In this work's case, the aim was to use a programme based on the Geant4 software, which is a software created to simulate the passage of particles through matter, which has as a base a set of physical models that allow the simulation of these passages in an extensive interval of energies. This presents a set of tools with a wide range of features such as geometry, physical models and tracking, as well as presents physical processes that cover several areas of physics. This program was created exploring engineering software and object oriented technology, implementing the coding language C++. The requirements necessary to the user analysed led to the creation of a high level design with a modular and hierarchical

structure that presents a unidirectional flux of dependencies. This led to the creation of categories and in turn to the concept of toolkit that implicates that the user can assemble his own program for his specific application [21].

In preference to the Geant4 software, it was intended to use the software TOPAS, which is a program based on Geant4, but programmed in a way to simplify its use [22].

TOPAS [22] stands for TOol for PArticle Simulation and it is based on the Geant4 Simulation toolkit, with the Geant4 built directly in TOPAS, allowing for advanced Monte Carlo simulation for radiotherapy without needing to install Geant4. The program wraps Geant4 to allow users to simulate without having to know C++. It is important to notice the program is not clinically approved so it should not be used as primary dose calculator for humans. It can however be used within the scope of this work, as the goals are purely academic and not to implement any treatments on humans.

The main purpose of TOPAS is to allow for 3D machine building and irradiation. This is achieved by writing the irradiation set up, particle beam and scorers wanted in a text file. All of these are considered parameters and require a 'Parent' to be defined (making them the Child of said parameter). By default, the Parent of all parameters is the World, which corresponds to the area of simulation and can be made of any material, defined by the user. In the case of this work, the material of the World was defined as air, to simulate the environment of the irradiation, and the main parameters where the geometrical components of the irradiation setup, a proton beam source and scorers to calculate the energy spectrum, dose and energy deposition. The simulation is more detailed in the later topic
Simulation setup.

In terms of physics list, the default from the program was the one used. This list includes 6 modules based of similar Geant4 modules, regarding standard physics, hadrons physics, decays, ion binary, hadron elastic physics and stopping physics. These modules were believed to be sufficient for this work, however, throughout the course of the work, it was noted that the resonance p-B reaction at 675 keV does not exist, and consequently does not include the release of three alpha particles for each incident proton. This file cannot be altered and through the course of the work I could not find a way to manually introduce a different cross section nor find files relative to proton elastic collisions.

Van de Graaff accelerator

This work was conducted at CTN/IST (Campus Tecnológico e Nuclear, Pólo de Loures do IST Estrada Nacional 10 (km 139,7), 2695-066 Bobadela LRS - Portugal), which is a Technological and Nuclear Campus from Universidade de Lisboa. In Figure 2 it is presented a schematic of the accelerators' laboratory at CTN.

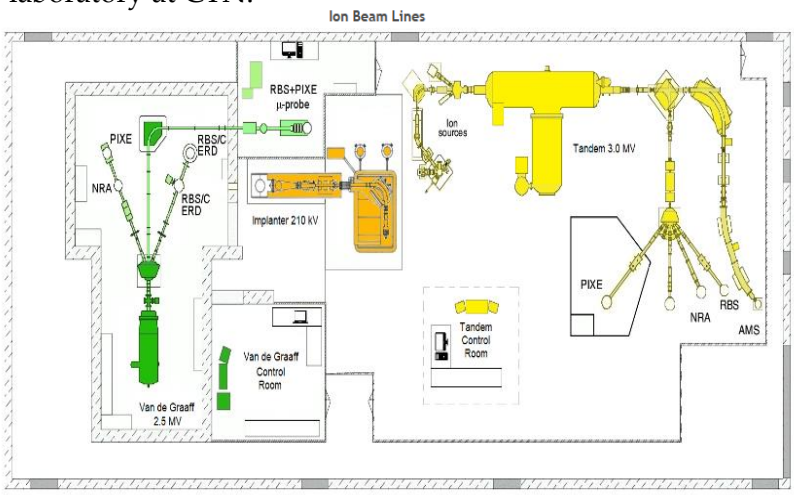

Figure 2 - Schematic of the ion beam lines at CTN-IST (from http://www.ctn.tecnico.ulisboa.pt/facilities/lfi/uk_experimental_hall.htm)

For this work, the accelerator used was the Van de Graaff accelerator, which is shown on the left side of Figure 2 (green colour). In principle, a Van de Graaff generator is an electrostatic generator that is composed by a moving belt of an isolating flexible material connected to the ground and to a metallic sphere. The movement of the belt allows for electric charge to be accumulated in the sphere, generating an electric potential [23]. The accelerator present at CTN is a AN-2500 Type-A model, fabricated by *High Voltage Engineering Europe* and, like the original, it is an electrostatic accelerator [24]. It is a horizontal one and has the capacity to 2.5 MV of tension in its terminals. This accelerator is inside a metallic cylinder that is pressurized with SF_6 and N_2, to help isolate it electrically and can produce positive ion beams with up to 2.5 MeV [24]. Just like Van de Graaff stated in is early works, this accelerator works better in vacuum [23]. This way, several primary and secondary vacuum pumps can be found along the accelerator, working to achieve a pressure of about 10^{-6} mbar. This accelerator is then divided in three different lines of work, which allow the use of different techniques. Figure 3 shows the three different lines:

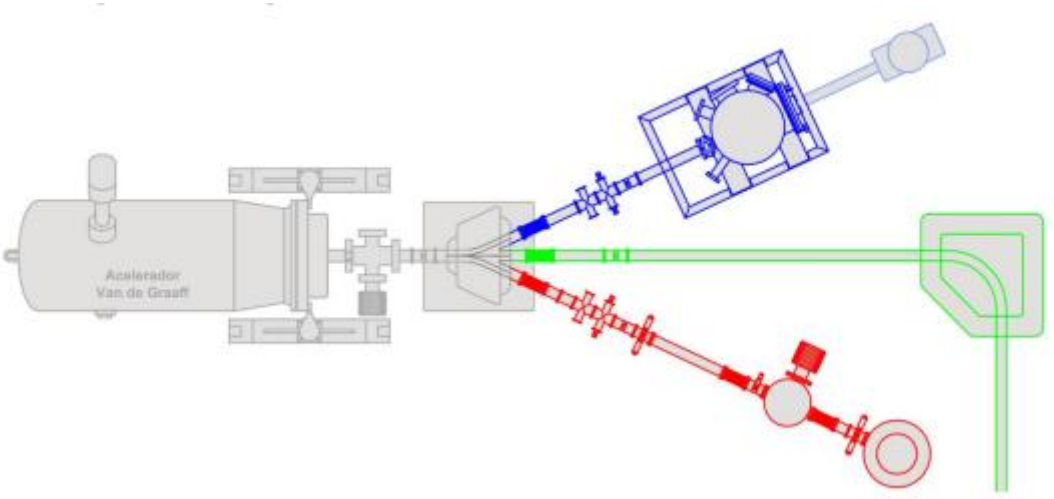

Figure 3 - Lines of work in the Van de Graaff accelerator

The one coloured in blue is used for JET/PIXE analysis, the red one for RBS and the green one is the microprobe, which was the one used in this work. The beam suffers a magnetic deflection in order to be directed to the one of the lines.

Microprobe

The microprobe's object aperture's size and the collimator aperture are defined by two sets of micrometre driven slits, which define beam current and beam divergence, respectively. These slits are made of tungsten and in Figure 4 are represented by OS (object slits) and CS (collimation slits). The microprobe also has scanning coils (SC) that are found right before the lenses. This lenses system (Q-lenses) is a high excitation magnetic quadrupole triplet and is used to focus the beam, both inside the chamber (S_1) and outside it (S_2). This lens system, the scanning coils, the collimator slits and the chamber are all on a concrete block, which in turn is on a layer of polystyrene to minimise the vibrations transmitted from the ground. The chamber is in vacuum, achieved using a diffusion pump, reaching a pressure of 10^{-6} mbar [24]. At the end of the chamber there is a nozzle (n) with a mylar window (My_n) of 6.3 μm thickness to support the pressure differences. In front of this nozzle there is a table for sampling position that can be moved along all three axis, x, y and z. There is also a minicamera to help with focus and positioning.

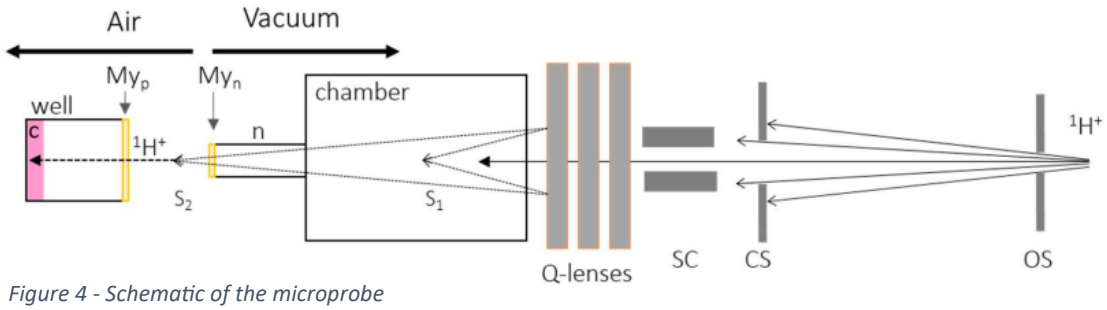

Figure 4 - Schematic of the microprobe

Experimental Setup

At the left side of Figure 4 it is represented the set up for cell irradiation. A plate with 96 wells (only one well is represented in the figure 4, to illustrate) is positioned at a 2.0 mm distance from the nozzle's end. The plate is covered in a 12.6 μm layer of mylar in the schematic (this layer is only used in half of the experiments, which will be explained later). The end of the layer is distanced 11.4 mm from the end of the plate, where the last 30.0 μm correspond to where the cells are. This way, when simulating, the goal was to have the particles cross 6.3 μm of mylar, 2.0 mm of air, another 12.6 μm of mylar, 11.37 mm of air and lastly 30.0 μm of water, which represent the cells.

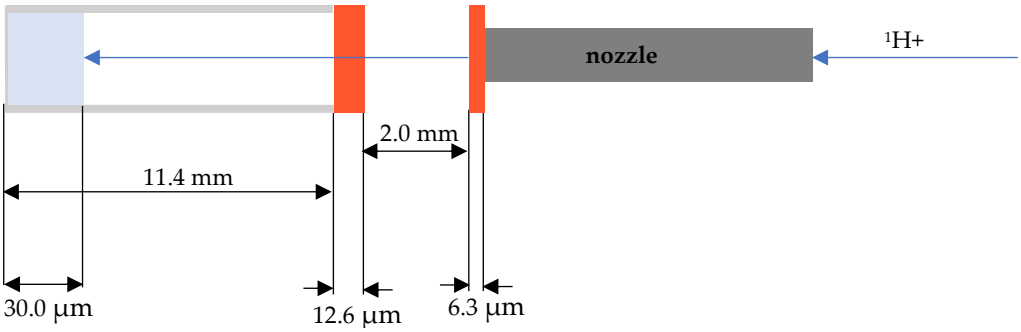

Figure 5 - Schematic of the irradiation set up

Simulation setup

The purpose of the simulations was to develop an irradiation model based on the experimental set up of proton irradiation (see previous section for experimental setup description) and validate the computational model with the proton beam characteristics. Under this framework, the goal was to simulate a 1.975 MeV proton beam passing the two layers of mylar, a layer of air and hitting the cells, like explained in the Experimental Setup (see Figure 5).

To build this environment, the World was defined as a cube with 1.6 mm of length and made of air. The two layers of mylar were built as TsBox with 6.35 mm of height and length and a thickness of 6.3 μm for the first layer and 12.6 μm for the second one. They were positioned within the World at x = 0.0, y = 0.0 and z = 7.99685 mm for the thinnest layer and z = 5.9874 mm for the thickest one, from the centre of the World, distanced between them 2.0 mm according to the experimental set up. A beam source was positioned at the edge of the World, behind both mylar layers, and with the particles following a trajectory along the Z axis. Figure 6 below shows the World (delimited by the white lines) and the two layers of mylar (drawn in red), as well as a few particles' trajectories, represented by the blue lines. The little red dots visible along the protons' trajectories represent scattered electrons.

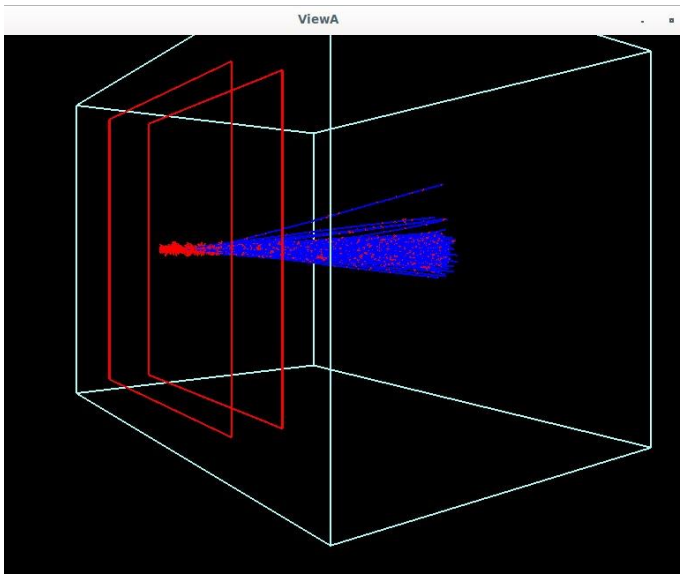

Figure 6 - View of a simulation

The last component in the simulation was the cell. At first, the cell simulated was a simple sphere made of water, with a 15.0 μm radius, positioned at the coordinates x = 0.0, y = 0.0 and z = -5.4039 mm, distancing the end of the cell from the last layer of mylar 11.4 mm. Because of the need to check both the dose in the cytoplasm and the nucleus of the cell, this geometry was altered to two concentrical spheres, one representing the cytoplasm with the 15.0 μm radius as the previous simulation, while the nucleus had only a 5.0 μm radius, so that there could be two different scorers. Four distinct types of two spheres geometries were tested, two where the cytoplasm and the nucleus were both children of the World and two where the cytoplasm was the Parent of the nucleus. In both scenarios two types of cytoplasm were drawn: one hollow in the middle, with the hollow part with the same dimensions as the nucleus and another where the cytoplasm was a full sphere with the nucleus inside it. After testing all four geometries, it was concluded that the right one for this work was the geometry

with the nucleus defined as a child of the cytoplasm which was in turn a complete sphere (not hollow).

As previously described, the $^{11}B(p, \alpha)\alpha\alpha$ reaction presents a resonance peak of alpha production at 675 keV of the primary proton beam energy. For this reason, it is important to know if the proton beam reaching the cells is near this energy value. In order to test this, a simulation in the conditions previously described was run with an Energy Spectrum calculated for both the nucleus and the cytoplasm. The initial energy of the beam was 1.975 MeV. The results of the spectrum can be found in Figure 7.

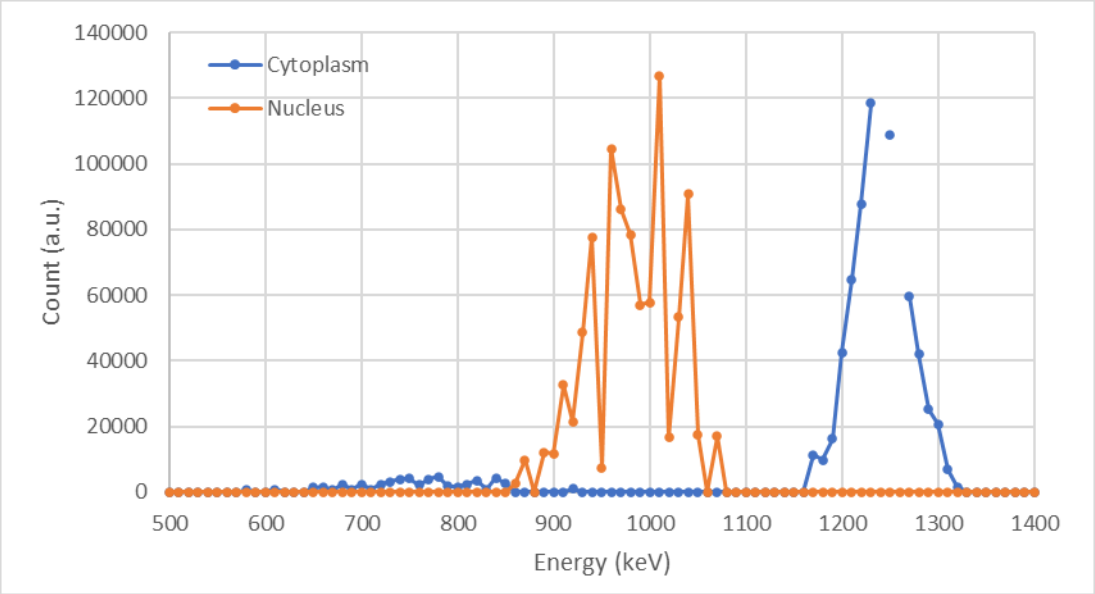

Figure 7 - Energy spectrums for simulated cytoplasm and nucleus

The x axis is the energy bins in keV and the y axis is counts. The program only analyses the energy of the particles on the surface of the components analysed. Looking closer at the zone of the graph where the 675 keV are, shown in Figure 8, we can see that this energy is reached, but only by a small percentage of the incident particles. The fact that there are no more energies lower than that also means this energy is reached at the end of the cell (considering the beginning the surface of the cell first hit by the proton beam).

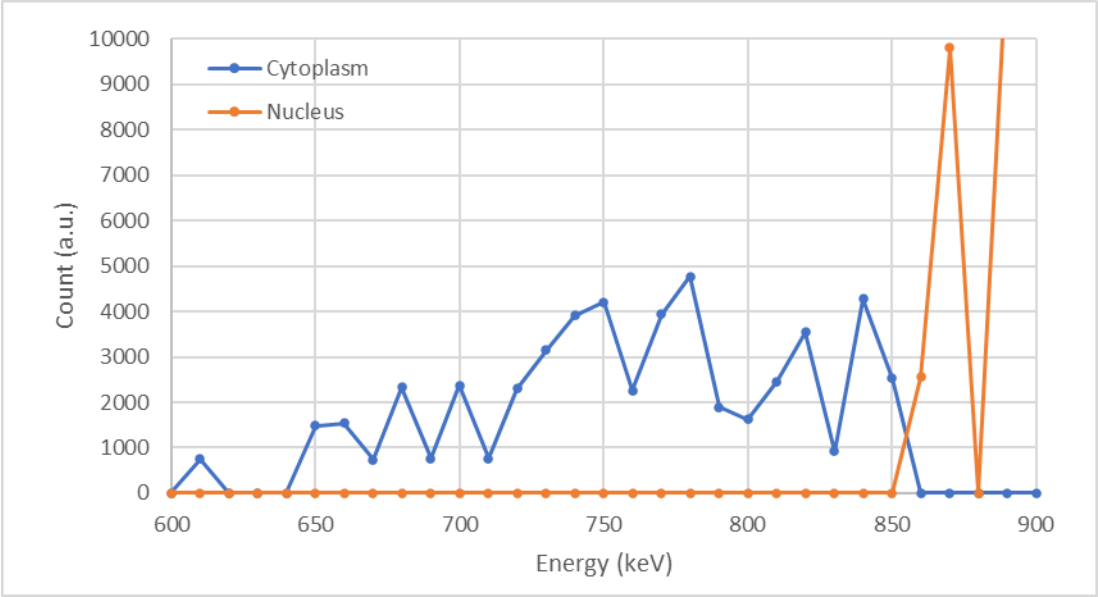

Figure 8 - Analysis of the energy spectrum with focus on the values of energy near the 675keV resonance peak value

After checking the energies, scorers where included: one for absorbed dose and one for deposited energy. By running a test in a simple sphere of water (without the cytoplasm and nucleus distinction), we verified the relation between dose and deposited energy. As we asked for these scorers, extra parameters were added. We requested both the sum and the mean for both scorers; the sum gives the total value of either dose or deposited energy, while the mean provides the value by particle. The dose (or deposited energy) per particle is a normalization and therefore makes it simpler to compare values from different programs and obtained experimentally. The simulations were all performed with a beam energy of 1.975 MeV and all had 50000 histories. The tests all kept the geometry previously explained except for the cell. For the simulation work three irradiation scenarios were considered:

1) nucleus and cytoplasm made of water, irradiated by the primary proton beam;
2) nucleus made of boron and cytoplasm of water, irradiated by the primary proton beam;
3) nucleus and cytoplasm made of water, with an isotropic source of alphas in the centre of the sphere.

This last simulation served as a verification of the increase in dose by the creation of alpha particles, forcing it this way, since no alphas were detected in the previous ones. The cell with a boron nucleus was simulated for five varied sizes of the boron sphere and in these simulations an extra scorer was added, OriginCount, to count if there were any alpha particles being generated. All simulations were later replicated without the second layer of mylar (the 12.3 μm thick layer). The full code for each parameter can be consulted in APPENDIX A and results of all the simulations can be found in RESULTS.

Radiobiology studies

The experimental part of this work consisted in irradiating tumour cells grown in a plate and verify their survival. To assess if the boron compound influenced the survival rate, three different kinds of samples were prepared for each irradiation: one without any compound, one with a concentration of 50 μM of compound and one with a concentration of 100 μM. Then, all three of these cells were exposed to three different conditions: irradiated with a beam with energy in the values of the resonance, another with energy higher than the resonance value (direct beam) and not irradiated. This creates four distinct groups of cells that we can use to compare (non-irradiated cells are technically the same for resonance and direct beam since they do not receive any radiation, however they are different samples and will therefore be counted separately so they will be considered different), shown in Table 1:

Table 1 – Breakdown of the samples to irradiate

Resonance	
Irradiated	Non-irradiated
Control (no compound)	Control (no compound)
50 μM	50 μM
100 μM	100 μM
Direct beam	
Irradiated	Non-irradiated
Control (no compound)	Control (no compound)
50 μM	50 μM
100 μM	100 μM

Two different sets of irradiations were performed in two distinct dates, one on 25/01/2023 and another on 04/05/2023. The differences between the experiments are summarized in Table 2.

Table 2 - Irradiations assumptions

Experiment Date	**25/01/2023**	**04/05/2023**
Cells	PC3 (prostate cancer cells)	MDA (breast cancer cells)
Beam Energy	1975 keV	1950 keV
Compound	COSANE	COSANE
Flux (p s^{-1})	8.49×10^6	6.68×10^6

For the first date, a plate of 96 wells was used and 24 wells had cell groups in them, 12 on one side, to be irradiated, and 12 on the other to serve has non irradiated controls. Despite only needing 12 different wells to accommodate all conditions of cells defined, as shown in Figure 9, we used 24 wells, since we split each considered "type" of cell between two wells, to both create more statistic and to reduce the uncertainty, since the beam is not stable (the fluence varies). Only the top 6 on each side had the second layer of mylar, meaning that the top six were considered 'resonance' while the bottom six were 'direct beam'. The scheme in Figure 9 helps visualize this.

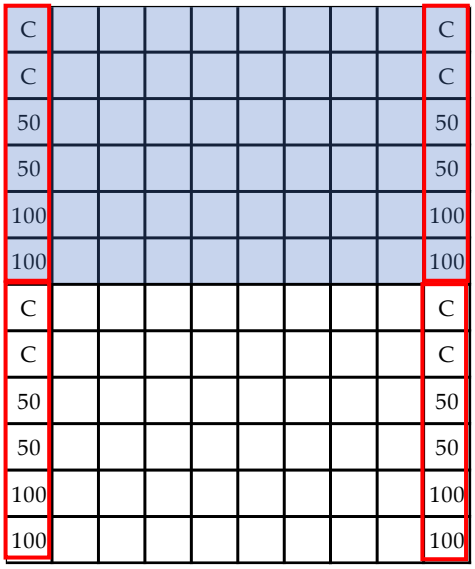

Figure 9 - Schematic of the 96 wells plate with the cell

The letter C represents the wells with cells without any compound (control) and the numbers are the concentration of compound present in the cells in that well. The blue layer represents the mylar. In the second experiment, the plates used had only 6 wells each, so each plate corresponded to one of the red rectangles in the scheme.

The experimental part can then be divided into three main parts: cell preparation, the irradiation and survival verification.

Cell preparation

The cells used were bought from a ATCC (American Type Culture Collection) and are preserved in liquid nitrogen, when not in use, and at approximately -80° C when in use. The cells were transferred from the flask at this temperature onto a bigger flask where they can perform mitosis (divide) to create more cells to use. To grow the cells, they were put in a medium of mostly DMEM with 10% fetal bovine serum and 1% of antibiotic solution (this is only added because these are experiments). When managing the cells, the environment must

be disinfected with alcohol of at least 70%. Before moving the cells onto the plates, these have to be sterilized using UV. After everything is properly disinfected, it is necessary to plate the cells onto the plates with the wells. The number of cells in each well depends on the size of the well, as the cells have a growth limit and can kill each other when out of space, which would influence the results in this work. Like mentioned before, for the first experiment (25/01/2023) the plates used had 96 wells whilst for the second one (04/05/2023) the plates used only had 6 wells each, but the methods used to adhere the cells were the same. To plate the cells, it is first necessary to count them. To do this, firstly the medium was removed. Then, the cells were washed with PBS (this has to be done quickly as PBS can alter the cells). After, trypsin was added to help release the cells that are attached to the bottom. Lastly, trypan blue solution was used to colour the cells; the dead cells turn blue while the living cells exclude the dye, allowing us to count only the living cells. A few drops of cells are then put into a grid scheme, like the one in Figure 10.

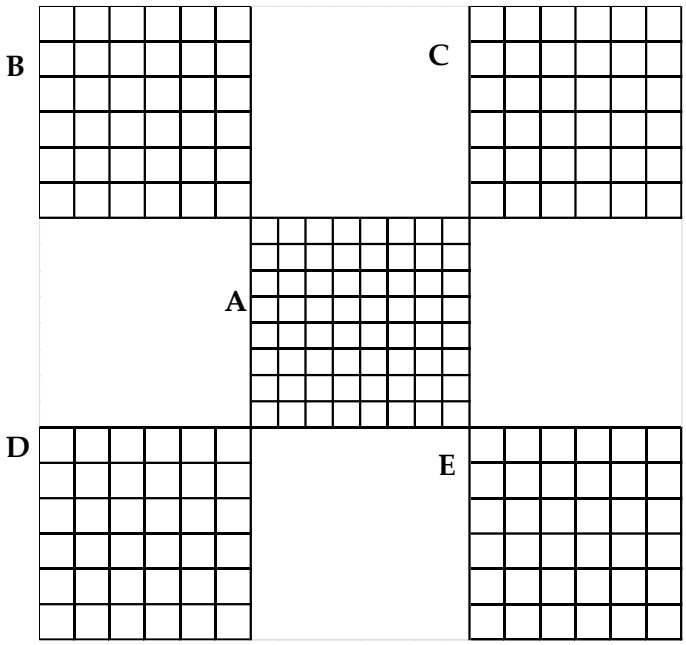

Figure 10 - Schematic of the grid for cell counting

The cells in the areas marked as B, C, D and E are counted separately and an average of the four gives the number of cells in 0.1 μL, since that is the volume of each one of the areas. This value is what will be used to calculate how many cells are in each well. These calculations are made based on proportions: we know how many cells there are in 0.1 μL, we know how many cells we want in the well, all we have to calculate is how many μL we need to take from the tube with the grown cells onto the well. The compound was then added in the adhered cells, and it is important to note that in the highest concentration used in this work, it has a rate of approximately 50% deaths, that is, it kills approximately half the cells.

This means that for an equal final number of cells, initially there had to be more cells with the compound. The cells were then incubated for 24 hours with more medium, duplicating in this time. They are then ready to be irradiated, after removing the medium, which should be done as closely to the time of irradiation as possible, since the cells naturally die without the medium.

Cell irradiation

The first step before starting irradiating was to focus the beam. This was done using the glass close to the nozzle and setting the scan to its maximum, regulating the voltage to an adequate value. After, we swept a Cu mesh 50 grid adjusting the nozzle so there was a full image of the grid. We then defined a mask for the sample sweeping. To measure the diameter of the beam, we used a fluorescent target of known size and take a picture of the full target with the light point, taking the size of the beam through the proportionality between the two. Lastly, we adjusted the current from the routine condition (~200 pA), closing the slits until we reach the desired count rate. The goal current value is between 1 pA and 5 pA. The current and fluence are estimated through RBS analysis of a golden target positioned inside the vacuum chamber (since there is no proton measurer in the air). After all these conditions were verified, we can initiate the actual irradiation. This was where the process differed for the two plates.

For the 96 well plate, because the wells are not much larger than the beam scan size, only one irradiation per well was done. The plate with cells (regardless of which one) was placed in front of the nozzle, at a 2.0 mm, just like explained in the Experimental Setup, with the beam centred in one of the wells in the corner. Then, for this sized plate, the accelerator is turned on and should hit the cells for 10 seconds in resonance (that is, when there is a second layer of mylar over the plate) and for 12 seconds for direct beam (when there is no mylar over the plate). This difference in time was theoretically calculated previously to ensure they receive the same dose. After the first irradiation time was finished, we moved the plate with the help of the x, y, z table onto the next well and repeated the process, until all wells we wish to irradiate had been irradiated.

For the 6 well plate, since the wells have a bigger diameter, instead of irradiating each well only once, we irradiated them four times each, to ensure we irradiated the biggest percentage of cells. Also, because of the size of the wells, before being brought to be irradiated, they were observed on a microscope to locate the cells and the plate was marked with a dot where the cells were, with a permanent marker, to help in the irradiation process. This way, using the laser present in the nozzle, which pointed to where the beam would hit the plate, and the camera, it was possible to “divide” the marked zone (so, the area where

there were cells) in four quadrants. We would point the laser to the centre of each quadrant, irradiate that zone, and then move do the next quadrant. Only after the well had been irradiated four times we would go to the next well. Figure 11 is a scheme to help represent the idea of the quadrants.

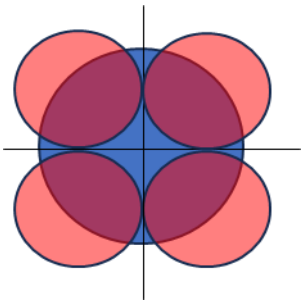

Figure 11 - Schematic of the irradiation of the 6 well plate

The blue circle represents the painted mark in the plate while the red circles represent the area irradiated each time. It is important to notice this was all done approximately and the plate was moved manually, so the accuracy is not the best. For this experiment, both the plate irradiated in the resonance and the plated irradiated by direct beam were irradiated for 10 seconds each time.

Cell survival assessment

The process of survival verification was different for the two sized plates. For the 96 wells plate, right after the irradiation, the cells were put in medium again and observed under the microscope to verify their condition. After, the medium was removed, the cells were washed with a saline solution and then trypsin was added to remove the cells from the bottom of the well. The cells from the irradiated controls (both together) were counted using a simple grid, like the one in Figure 12.

A	0				
0	X				
B	0				

Figure 12 - Schematic of the grid for cell count

The total number of cells per microlitre was given by the sum of counted cells (represented in the scheme by the letters), divided by the total number of squares and multiplied by two correction factors, the liquid factor and the correction factor from the microscope. So, we get:

$$[cells/\mu L] = \frac{number\ of\ cells}{squares} \times 2 \times 90, \text{ where } number\ of\ cells = A + B + X + \cdots.$$

The cells were then moved to petri plates with new medium. Every two wells that were joined (the wells in the same conditions of compound and irradiation) were split through three different petri plates, again to create more statistic and try to reduce the uncertainty. The cells were then incubated for about 14 days. The medium had to be changed halfway through this time since it loses its properties with time.

After waiting for 14 days, the cells were washed with a diluted PBS solution, and we used a fixing solution of three parts methanol to one part acetic acid to fix the cells in the petri plate. The petri plates with the fixing solution were left resting for 15 minutes, time after which the fixing solution was removed and the petri were left to dry. Once they were completely dry, we introduced a buffer solution with some dye, covering the entire petri dish and left that to rest for 8 minutes. After this time ended, we removed the liquid and washed the plates in the sink. The cells were then coloured and adhered to the plate, making it easier to count them.

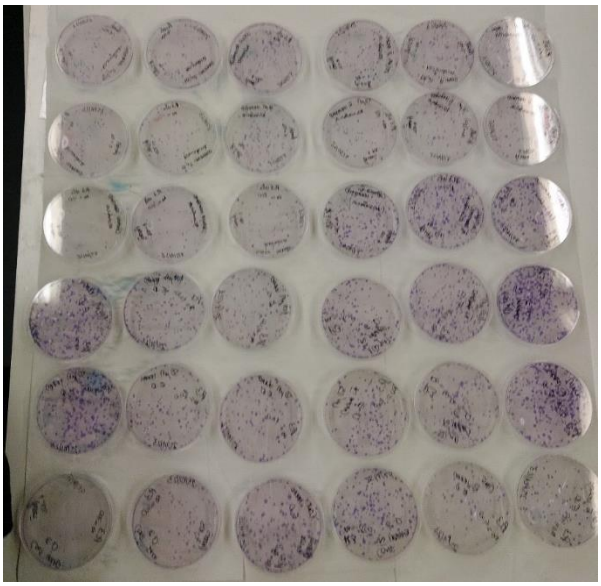

Figure 13 – Petri dishes with the cells after colouring

The number counted was, however, not the number of cells, but the number of colonies. A colony is a group of cells with at least 50 cells. The colonies are mostly visible by naked eye when coloured and, when in doubt, a microscope was used to verify if the group was big enough to be a colony or not. The counting process was manual for all 36 petri plates and the results were annotated.

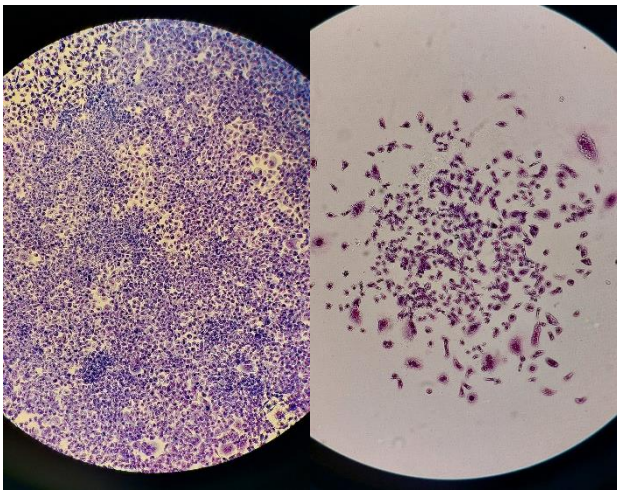

Figure 14 - A big colony (on the left) and a smaller colony (on the right) observed under a microscope

For the 6 wells plates, the cells did not need to be moved to petri dishes since the wells were big enough to allow the growth of the cells, so the new medium was added directly here, and they were left to incubate for the same 14 days. However, there was an issue, and the cells were not counted by the end of this time period. This will be further explained in the Results section.

4

RESULTS

In order to have base values to compare the experimental data to, we calculated the energy deposited in one cell theoretically. Considering a beam of protons with 1975 keV that goes through 6.3 μm of mylar, then 1.1 cm of air and again 12.3 μm of mylar, it will lose energy before reaching the cell. To calculate this loss of energy, all stopping power values were obtained from NIST, considering the proton's initial energy and the material it would cross. The densities considered for each material can be found in A.1 Densities. The calculations were also made for the direct beam irradiations, where we only have one layer of mylar and one layer of air and the results can be found in Table 3.

Table 3 - Proton energy loss before reaching the cell

Resonance conditions			**Direct beam**		
Initial energy	Stopping power	Layer material and thickness	Initial energy	Stopping power	Layer material and thickness
1.975 MeV	147.9 MeVcm²/g	Mylar 6.3 μm	1.975 MeV	147.9 MeVcm²/g	Mylar 6.3 μm
1.846 MeV	145.2 MeVcm²/g	Air 0.2 cm	1.846 MeV	145.2 MeVcm²/g	Air 1.33 cm
1.810 MeV	157.6 MeVcm²/g	Mylar 12.3 μm	Final energy = 1.609 MeV		
1.536 MeV	165.5 MeVcm²/g	Air 1.13 cm			
Final energy = 1.307 MeV					

This means that, after the irradiations, the energy that reaches the cell is 1307 keV with the extra layer of mylar and 1609 keV without it. We can now calculate an approximation of the dose the cell receives in both cases. This is only an approximation because we are considering the stopping power to be constant throughout the whole cell and this is not true. However, since the cell is spherical and we are considering the distance travelled by the particle as the diameter, we are not considering some particles will travel less and will therefore deposit a higher energy, so in first approximation this calculation should not be far from the real value. The results of this calculations can be found in Table 4.

Table 4 - Proton energy loss while crossing the cell

Resonance conditions			**Direct beam**		
Initial energy	Stopping power	Layer material and thickness	Initial energy	Stopping power	Layer material and thickness
1.307 MeV	216.0 MeVcm²/g	Water 30 μm	1.609 MeV	186.0 MeVcm²/g	Water 30 μm
Final energy = 0.659 MeV			Final energy = 1.051 MeV		

This proves that, in the resonance conditions, the resonance value in boron (0.675 MeV) is reached inside the cell. The schematic in Figure 15 helps visualise the proton's energy loss during its path, in resonance conditions (for direct beam the process is similar, but with one less layer of mylar), where the blue dots represent the proton before the material of the medium changes, and it is written the energy it has in each of these points.

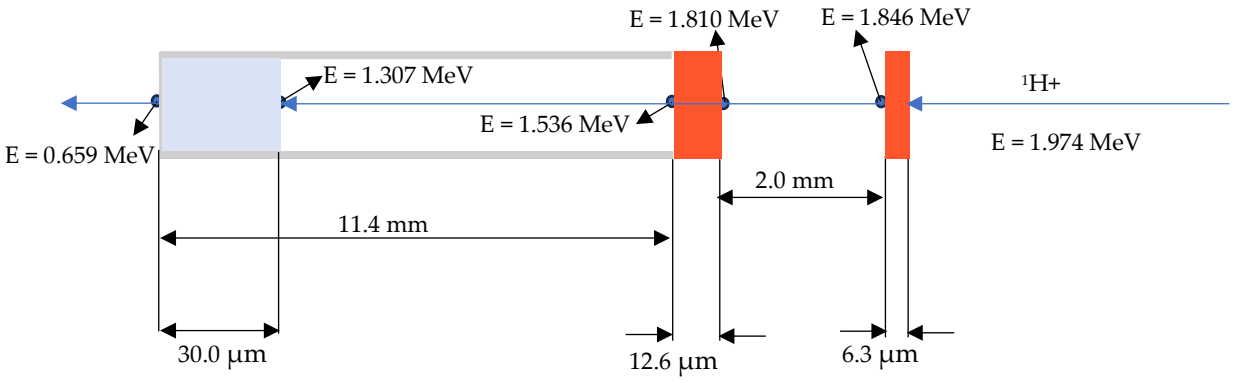

Figure 15 - Schematic of the irradiation set up with proton's energy

To calculate the dose, we considered the energy lost during the protons crossing of the cell (same valued calculated before that subtracts from the initial energy to get the energy after leaving the cell), we converted it to joule and divided by the mass of a cell in kilograms, giving the final result in Gy (=J/kg). Since we are considering the cell as a sphere of water with a 15 μm radius, its mass is:

$$Cell\ mass = \frac{4}{3}\pi(15 \times 10^{-4})^3 \times \rho = 1.4\ \times 10^{-8}\ g \qquad (1)$$

The dose for the cells irradiated in the resonance will then be:

$$Dose = \frac{0.648\ \times 10^{6} \times 1.6\ \times 10^{-19}}{1.4\ \times 10^{-8}\ \times 10^{-3}} = 0.0074\ Gy = 7.4\ mGy/p \qquad (2)$$

Where 0.648 = 1.307 – 0.659 is the energy a proton loses while crossing the cell, in MeV, 10^6 is the conversion to eV and $1.6\ \times 10^{-19}$ is the conversion factor to J.

For the cells irradiated with direct beam the energy lost by a proton will be 0.558 = 1.609 – 1.051. So, analogously:

$$Dose = \frac{0.558 \times 10^{6} \times 1.6 \times 10^{-19}}{1.4 \times 10^{-8} \times 10^{-3}} = 0.0064\ Gy = 6.4\ mGy/p \quad (3)$$

Since we are only considering the energy of one proton, the doses obtained are per particle, that is, Gy per proton.

To normalize the dose obtained to a dose per cell, to compare with the other results, obtained through simulations and experiments, it was necessary to calculate the number of protons per cell. With the data from the experiment, we can obtain the number of protons that each cell receives. If we multiply this value by the dose per proton, we can have a dose per cell. Table 5 reports the experimental data that permitted to estimate the proton flux in terms of number of protons/cells, and that were used to normalize the theoretical absorbed dose, obtained through equation 2.

Table 5 – Calculation of number of protons per cell

	25/01/2023	**04/05/2023**
Flux density (p cm^{-2} s^{-1})	1.05×10^{8}	4.60×10^{7}
Cell area (cm^2)	7.07×10^{-6}	
Irrad time (s)	10	
Protons/cell	7.46×10^{3}	3.25×10^{3}

Since the theoretical absorbed dose obtained through equation 2 is a dose per proton (Gy/p), multiplying the number of protons per cell reported in Table 5, we obtain the final dose of 55.2 Gy and 24.1 Gy, considering both irradiations, chronologically.

Simulations

As mentioned previously, all TOPAS simulations were run in the conditions of a beam with 1.975 MeV energy, in air, with a geometry equal to the experimental setup, with a cell of maximum size equal to 30 μm radius and had 50 000 runs.

To do the simulations with the boron nucleus as faithful as possible to the experimental conditions (considering they are already different, since in these simulations the boron is condensed in one point instead of spread throughout the cell), the amount of boron in a cell was taken into consideration. It was estimated that for each gram of cell, there were 68 μg of ^{11}B (when considering 50 μM of COSANE concentration). Considering a cell has a diameter of 30 μm and is made of water, its total mass is 1.414×10^{-8} g. This means, in total, a

cell has 9.613×10^{-13} g of ^{11}B. Dividing this value by the density of the boron, we get the total volume of boron in the cell, 4.108×10^{-13} cm^3. Since we are building a sphere of boron in the centre of the cell, we take into consideration the formula for the volume of the cell and get a radius of 4.612×10^{-5} cm which is equal to 0.4612 μm. Table 6 shows the results of the simulation of a cell made entirely of water, without a nucleus, Table 7 shows the results for a cell also made of only water, but with the differentiation between nucleus and cytoplasm, Table 8 shows the result of the simulations for a nucleus made of boron and Table 9 show the results for a boron nucleus with the radius calculated considering the real estimated concentration.

Table 6 - Results of the simulations without a nucleus

	Resonance Conditions	**Direct Beam**
Dose per proton (Gy/p)	6.482×10^{-6}	1.442×10^{-5}
Energy Deposited per proton (MeV/p)	5.720×10^{-4}	1.273×10^{-3}

Table 7 - Results of the simulations with a water nucleus

	Resonance Conditions		**Direct Beam**	
	Cytoplasm	Nucleus	Cytoplasm	Nucleus
Dose per proton (Gy/p)	6.611×10^{-6}	4.819×10^{-6}	1.441×10^{-5}	1.386×10^{-5}
Energy Deposited per proton (MeV/p)	5.617×10^{-4}	1.575×10^{-5}	1.225×10^{-3}	4.529×10^{-5}

Table 8 - Results of the simulations with a 10 μm diameter boron nucleus

	Resonance Conditions		**Direct Beam**	
	Cytoplasm	Nucleus	Cytoplasm	Nucleus
Dose per proton (Gy/p)	6.688×10^{-6}	4.253×10^{-6}	1.459×10^{-5}	1.199×10^{-5}
Energy Deposited per proton (MeV/p)	5.683×10^{-4}	3.253×10^{-5}	1.239×10^{-3}	9.170×10^{-5}

Table 9 - Results of the simulations with a 10 μm diameter water nucleus and a 0.4612 μm radius boron sphere in the centre

	Resonance Conditions		**Direct Beam**	
	Cytoplasm	Nucleus	Cytoplasm	Nucleus
Dose per proton (Gy/p)	6.611×10^{-6}	4.819×10^{-6}	1.441×10^{-5}	$1.386E^{-5}$
Energy Deposited per proton (MeV/p)	5.617×10^{-4}	1.575×10^{-5}	1.225×10^{-3}	$4.529E^{-5}$

The next three tables, Table 10, Table 11 and Table 12, present the results of simulations when varying the size of the boron nucleus. This was performed as a sensitivity test to verify the impact of dose variation with the change on volumetric percentage of boron.

Table 10 - Results of the simulations with a 2 µm diameter boron nucleus

	Resonance Conditions		**Direct Beam**	
	Cytoplasm	Nucleus	Cytoplasm	Nucleus
Dose per proton (Gy/p)	6.484×10^{-6}	0	1.442×10^{-5}	1.166×10^{-5}
Energy Deposited per proton (MeV/p)	5.719×10^{-4}	0	1.272×10^{-3}	7.136×10^{-7}

Table 11 - Results of the simulations with a 5 µm diameter boron nucleus

	Resonance Conditions		**Direct Beam**	
	Cytoplasm	Nucleus	Cytoplasm	Nucleus
Dose per proton (Gy/p)	6.512×10^{-6}	0	1.445×10^{-5}	1.394×10^{-5}
Energy Deposited per proton (MeV/p)	5.719×10^{-4}	0	1.269×10^{-3}	1.333×10^{-5}

Table 12 - Results of the simulations with a 20 µm diameter boron nucleus

	Resonance Conditions		**Direct Beam**	
	Cytoplasm	Nucleus	Cytoplasm	Nucleus
Dose per proton (Gy/p)	6.611×10^{-6}	4.819×10^{-6}	1.441×10^{-5}	1.386×10^{-5}
Energy Deposited per proton (MeV/p)	5.617×10^{-4}	1.575×10^{-5}	1.225×10^{-3}	4.529×10^{-5}

Like mentioned previously, for all the simulations where boron was used, a scorer called OriginCount was introduced to verify the formation of alpha particles, as it would return the number of alpha particles counted in the cell during the irradiation. However, the obtained count was always zero.

To calculate the total dose, it is necessary to know the total number of protons to consider. Considering that the time variable as no impact in the simulations, since it was not considered, instead of using the number of protons, it was used the calculated flux from the experiments.

Considering the dose obtained in the simulations does not vary much with the parametrization, the value considered for the calculations is the one most similar to the experiment, present in Table 9, averaging the values obtained for dose in the nucleus and cytoplasm, obtaining a dose equal to 5.715×10^{-6} Gy/p. Multiplying this dose by the flux, for both dates, we obtained the total dose values presented in Table 13.

Table 13 - Dose calculations for simulation setup

	25/01/2023	**04/05/2023**
Experimental flux (p/s)	8.49×10^6	6.68×10^6
Dose (Gy/p)	5.715×10^{-6}	
Dose (Gy)	48.5	38.2

The simulation of 100 alpha particles with an energy of 3.0 MeV each gave the following results, present in Table 14, for dose and energy deposited per particle:

Table 14 - Results of the simulations with an isotropic alpha source

	100 alphas with 3.0 MeV
Dose per alpha particle (Gy/α)	3.156×10^{-2}
Energy Deposited per alpha particle (MeV/α)	2.784

The proton boron fusion reaction emits one alpha particle with 3.76 MeV and two others with 2.74 MeV[8]. For the simulations, a rounded average energy of 3.0 MeV was used. To know the number of alphas expected, we calculated the yield of the reaction, considering the experimental conditions. Knowing the estimated boron quantity of 68 μg/g, assuming the cell diameter equal to 30 μm, the density of water as 1 g/cm^3 and the approximate cross section of the proton boron fusion reaction as 1 barn, we get a yield of 1.1×10^{-8}.

$$Y = 10^{-24} \times 68 \times 30 \times 10^{-4} \times \frac{6.023 \times 10^{23}}{11 \times 10^6} = 1.1 \times 10^{-8} \qquad (4)$$

where $\frac{6.023 \times 10^{23}}{11 \times 10^6}$ is the Avogadro constant over the atomic mass of boron, in μg. Since this gives the number of interactions per proton, if we multiply by the number of protons and then by 3, considering each interaction generates 3 alpha particles, we get the total amount of alphas created.

$$1.1 \times 10^{-8} \times 1.26 \times 10^9 \times 3 = 41.58 \qquad (5)$$

This is, however, considering the total number of protons in the irradiation. To make a more accurate simulation, considering only one cell is being simulated, the number of protons per cell was calculated, as can be found in Table 5. The value obtained was 7.46×10^3 protons per cell, for the first date of experiments. This means there is less than 1 alpha being generated in each cell.

$$1.1 \times 10^{-8} \times 7.46 \times 10^3 \times 3 = 2.46 \times 10^{-4} \qquad (6)$$

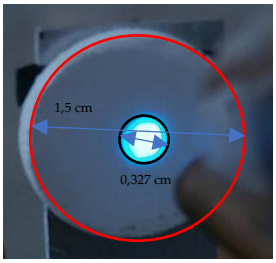

Figure 16 - Picture of the beam in fluorescent target

For the irradiations performed on the 25/01/2023:

To measure the diameter of the beam, two circles were drawn over the picture of the beam hitting the fluorescent target, both for the target and the beam. The measurements obtained represented a ratio of 4.5 vs 1.09. Since we know the target has a diameter of 1.5 cm, we conclude that the beam sweeping area has a 0.327 cm diameter, meaning the sweeping area is 0.0869 cm^2. Considering the area of one well is 0.32 cm^2, this means 43.5% of the well was irradiated. Multiplying the irradiated area by the cell thickness (considering the diameter, 30.0 μm) we get the irradiated mass per well, which is equal to 2.61×10^{-7} kg.

After this, it is necessary to analyse the data retrieved through the program of the microprobe. It outputs a file that condenses the information of the runs of the gold RBS. From this file, we take the raw charge, in nC, the Q factor (it is a factor that normalizes charge for RBS) and the time of each run. By multiplying the raw charge (converted to C) by the Q factor and dividing by the elemental charge we obtain the number of protons (Equation 7). If we divide this result by the time of the run we get the number of protons per second, which is, the flux[2] (Equation 8). We then do an average of the results from all runs. We can also calculate the flux density2, dividing the flux by the irradiated area (Equation 9).

$$\frac{raw\ Q \times 10^{-9} \times Q}{1.60 \times 10^{-19}} = number\ of\ protons \qquad (7)$$

where 10^{-9} is the conversion from nC to C and 1.60×10^{-19} is the proton elemental charge.

$$\frac{number\ of\ protons}{time} = flux \qquad (8)$$

$$\frac{flux}{0.086935} = flux\ density \qquad (9)$$

where 0.086935 is the irradiation area, in cm^2. The data outputted by the program can be found in APPENDIX B, where it is also presented the calculated flux and flux density for that date, which were 8.46×10^6 p s^{-1} and 1.05×10^8 p cm^{-2} s^{-1}, respectively.

After knowing the average flux, and since we also know the LET, as it was previously obtained through the use of the program SRIM, in eV per μm, we can calculate the dose. We multiplied the LET by the cell thickness to get the total energy, and then multiplied this value by the number of protons per second (the flux) and by the conversion of keV to J. The dose was then obtained by dividing the obtained value by the irradiated mass. To get the total

[2] The definitions of flux, flux density and fluence can be found in annex A.2 Definitions of flux, flux density and fluence

dose, we multiplied by the irradiation time. This was done for the cells with the two mylar layers.

$$Dose = \frac{LET \times 30\mu m \times flux \times 1.60 \times 10^{-16}}{mass} \times time \quad (10)$$

For the direct beam irradiations, to calculate the dose, we use the flux, multiply by the LET, by a factor of 10000 to convert to cm, by the conversion of keV to J and then divide this result by the density of water.

$$Dose = \frac{flux \times LET \times 10000 \times 1.60 \times 10^{-16}}{\rho} \times time \quad (11)$$

The results are shown in Table 15:

Table 15 - Dose calculations for the first irradiation

Conversion keV to J 1.60E-16
Irradiated mass (kg) 2.61E-7
With Mylar 12.6 um

Cell thickness (μm)	LET (keV/μm)	Energy (keV)	Energy rate (keV/s)	Dose rate (Gy/s)	Irrad time (s)	Dose (Gy)
30	26.433	793.0	1.08 x10^{-6}	4.14	10	41.4

ρ(H2O) = 1 g/cm^3

ρ(H2O) kg/cm^3	0.001

Direct beam

Cell thickness (μm)	LET (keV/μm)	Dose rate (Gy/s)	Irrad time (s)	Dose (Gy)
30	21.633	3.66	12	43.9

Like explained in the Cell survival assessment topic, after incubating for 14 days, the cells where manually counted. Normalizations of the results of those counts are presented in Figure 17 and Figure 18. N0 is the initial number of cells in the petri dish.

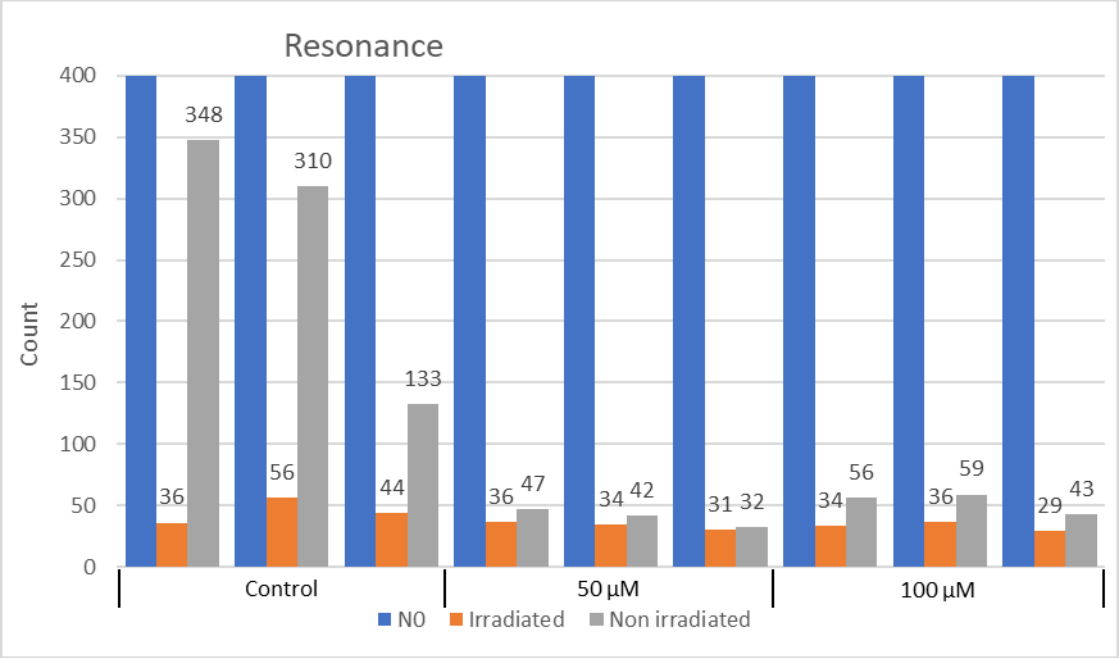

Figure 17 - Cell survival count in resonance conditions

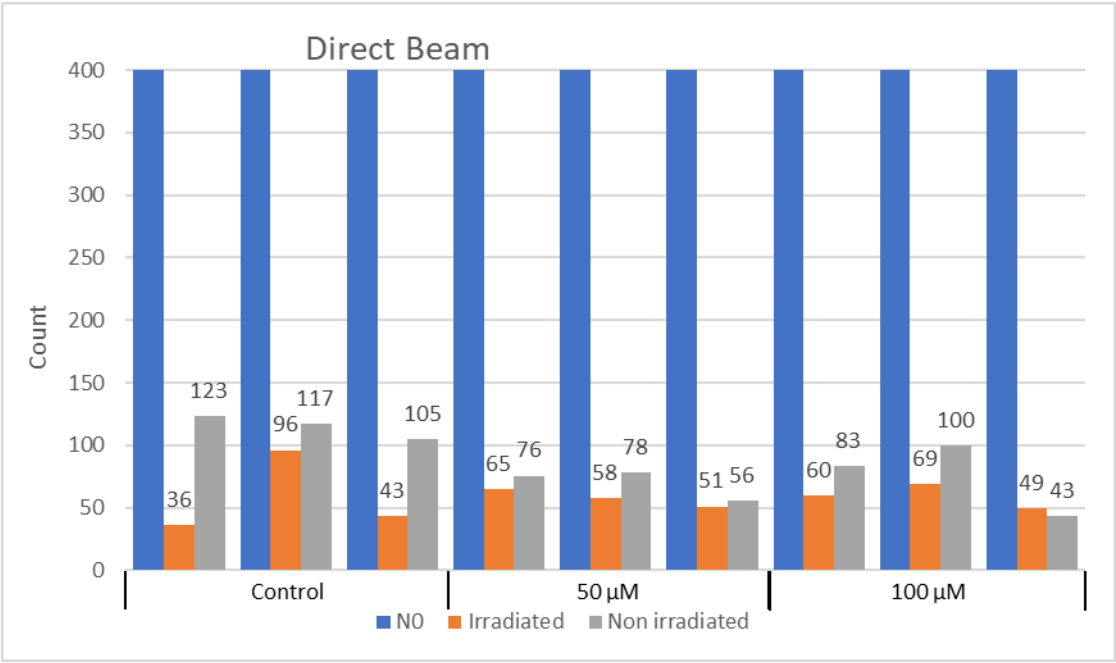

Figure 18 - Cell survival count in direct beam conditions

By looking at the graphics, we can quickly conclude that the results are against what was expected. The compound has a toxicity that kills about 50% of the cells in its highest concentration, however, we can see that the survival percentage was much lower than that, particularly looking at the non irradiated cells. Also, the non irradiated cells without compound (control) should have an almost 100% survival, however, in the graphic for the direct beam conditions, we can see that there was registered only about 30% survival. These results mean that the test is not viable and there was most probably an issue with some part of the trial. Analysing the results from the resonance conditions as well, the high survival of the non irradiated control cells is visible, but there was very low survival in the irradiated control cells. This means the irradiation, even without the compound, already applies a dosage that

causes a significative cellular death, which in turn can make it harder to identify the effects of the usage of the compound.

For the irradiations performed on the 04/05/2023:

The procedures were the same has mentioned before for the other date. The irradiated area had a diameter of 0.43 cm, which means its area was 0.14522 cm^2. The mass irradiated was $4.36x10^{-7}$ kg. This time, instead of taking the raw charge and the Q factor and multiplying them manually, the value taken of the program was already the result. The calculations were made using equations 7 and 8, with the obtained charge in Equation 7 instead of the raw charge times the Q factor and can be found in APPENDIX B. The obtained flux was $6.68x10^{6}$ p s^{-1}.

For this experiment, only the dose of the cells irradiated with the second layer of mylar was calculated. These calculations were made based on equation 10 and the results can be found in Table 16.

Table 16 - Dose calculations for the second irradiation

Conversion keV to J $1.60x10^{-16}$
Irradiated mass (kg) $4.36x10^{-7}$
With Mylar 12.6 um

Cell thickness (μm)	LET (keV/μm)	Energy (keV)	Energy rate (keV/s)	Dose rate (Gy/s)	Irrad time (s)	Dose (Gy)
30	31.2	936.0	$1.00x10^{-6}$	2.30	10	23.0

As for the results of the survival verification, after the 14 days period was over, there were no cells on the petri dishes after they were coloured, so after microscope observation it was concluded there was no survival, for any of the irradiated plates. Because there were no results, the non-irradiated were also not counted, as they were only control and there was nothing to compare them with.

5

DISCUSSION AND CONCLUSIONS

Looking at the results from the MC simulations, even though there are some minor differences when the boron is introduced, they are not significant, as the order of magnitude is the same. Therefore, our MC results do not support the radiosensitizing effect due to the presence of the ^{11}B. It is worth to say that this issue is still quite controversial, and while some experimental studies report the radio sensitizing effects due to the p - ^{11}B reaction [9], there are also several studies (experimental and theoretical) that show no radiosensitizing effect when ^{11}B is considered in proton irradiation setups[25][26]. The MC simulations without forcefully inducing the alpha particles do not show any alpha formation, which is coherent with the lack of changes in the absorbed dose. This is due to the fact that the Geant4 libraries included in TOPAS version used for this Thesis work, as mentioned previously, does not include the resonance p-B reaction at 675 keV.

From the dosimetric point of view, the MC simulations results were compared with the ones obtained with other two methods (empirical and theoretical). All the absorbed dose comparison can be found resumed below in Table 17:

Table 17 - Comparison of absorbed doses

	25/01/2023	**04/05/2023**
Theoretical dose (Gy)	55.2	24.1
Simulated dose (Gy)	48.5	38.2
Experimental dose (Gy)	41.4	23.0
Simulated alpha Dose (Gy)	8.36×10^{-2}	3.64×10^{-2}

Comparing all results obtained, by the experimental calculations, calculated theoretically and simulated, we can see they have the same order of magnitude, and therefore support each other.

Looking at the production of alpha particles per cell, we can see that it is very reduced and therefore the dose addition that results of the alpha production from the boron proton fusion reaction has no relevant impact in the total dose, being three orders of magnitude smaller than the dose obtained solely from the irradiation with a proton beam.

In terms of the results from the survival experiments, for the first one the values ended up being disregarded, because the method used to change the cells from the plate with the wells to the petri dishes introduced too many uncertainties: firstly, only less than half of the cells were irradiated, and out of the total only a very small number was then transferred to the petri dishes. This means that the chances of only having cells that were not irradiated were high. Also, in the process of washing the cells after the irradiation, the cells that had died immediately when irradiated were removed, therefore not entering the count, as they should. As mentioned before, the results of the second experiment were inexistent. One possible explanation could be due to the high dose to which cells were exposed (taking to cellular death), however this effect is highly masked by the several experimental problems encountered during measurement, both for cells handling and for the instability of the proton beam in irradiation setups.

The boron proton fusion reaction was not simulated due to the lack of the resonance peak cross section in the TOPAS code. However, with the combination of the theoretical calculations of alpha production and the simulation of an isotropic alpha source, it was possible to conclude that, in these conditions, the alpha particles have an irrelevant impact in the dose administrated in a cell through irradiation with a proton beam, being this result in agreement with literature [25]. In conclusion, we had no experimental results to verify the impact of the COSANE compound in cell irradiation, since several experimental problems were encountered during measurements, introducing in this way a lot of uncertainties and bias.

However, the MC model here developed permitted to assess absorbed doses with proton beam irradiations at the Van de Graaff accelerator (C2TN, Lisbon) and the two-step MC simulations with protons and alphas permitted also to assess the contribution of the alpha particles generated by the p-^{11}B reaction that, in agreement with literature, has no dose enhancement effect. Several other experiments will be necessary to better understand the radiosensitizing effect of ^{11}B that appear to be a complex process that probably cannot be explained only with the eventual production of alpha particles, but other reasons should be investigated, such as ^{11}B biochemical properties, uptakes and cell types, among others.

BIBLIOGRAPHY

[1] "The top 10 causes of death." Accessed: Sep. 29, 2023. [Online]. Available: https://www.who.int/news-room/fact-sheets/detail/the-top-10-causes-of-death

[2] "Cancer." Accessed: Sep. 29, 2023. [Online]. Available: https://www.who.int/news-room/fact-sheets/detail/cancer

[3] R. J. Goodburn *et al.*, "The future of MRI in radiation therapy: Challenges and opportunities for the MR community," *Magn Reson Med*, vol. 88, no. 6, pp. 2592–2608, Dec. 2022, doi: 10.1002/mrm.29450.

[4] S. Gianfaldoni, R. Gianfaldoni, U. Wollina, J. Lotti, G. Tchernev, and T. Lotti, "An overview on radiotherapy: From its history to its current applications in dermatology," *Open Access Maced J Med Sci*, vol. 5, no. 4 Special Issue GlobalDermatology, pp. 521–525, 2017, doi: 10.3889/oamjms.2017.122.

[5] D. K. Yoon *et al.*, "Application of proton boron fusion to proton therapy: Experimental verification to detect the alpha particles," *Appl Phys Lett*, vol. 115, no. 22, Nov. 2019, doi: 10.1063/1.5128953.

[6] "Current status of neutron capture therapy," 2001.

[7] J. Y. Jung, D. K. Yoon, B. Barraclough, H. C. Lee, T. S. Suh, and B. Lu, "Comparison between proton boron fusion therapy (PBFT) and boron neutron capture therapy (BNCT): A monte carlo study," *Oncotarget*, vol. 8, no. 24, pp. 39774–39781, 2017, doi: 10.18632/oncotarget.15700.

[8] D. K. Yoon, J. Y. Jung, and T. S. Suh, "Application of proton boron fusion reaction to radiation therapy: A Monte Carlo simulation study," *Appl Phys Lett*, vol. 105, no. 22, Dec. 2014, doi: 10.1063/1.4903345.

[9] G. A. P. Cirrone *et al.*, "First experimental proof of Proton Boron Capture Therapy (PBCT) to enhance protontherapy effectiveness," *Sci Rep*, vol. 8, no. 1, Dec. 2018, doi: 10.1038/s41598-018-19258-5.

[10] M. C. Spraker *et al.*, "The 11B(p,α) 8Be $\rightarrow$ α + α and the 11B(α,α) 11B Reactions at Energies Below 5.4 MeV," *Journal of Fusion Energy*, vol. 31, no. 4, pp. 357–367, Aug. 2012, doi: 10.1007/s10894-011-9473-5.

[11] A. Pelaghia, G. Crete, and A. G. Ruggiero, "Contribution to Conference on Prospects for Heavy Ion Inertial Fusion Nuclear Fusion of Protons with Boron."

[12] C. D. Willey, E. S. H. Yang, and J. A. Bonner, "Interaction of Chemotherapy and Radiation," *Clinical Radiation Oncology*, pp. 63-79.e4, Jan. 2016, doi: 10.1016/B978-0-323-24098-7.00004-6.

[13] H. Murshed, "Radiation Biology," *Fundamentals of Radiation Oncology*, pp. 57–87, Jan. 2019, doi: 10.1016/B978-0-12-814128-1.00003-9.

[14] S. Gavas, S. Quazi, and T. M. Karpiński, "Nanoparticles for Cancer Therapy: Current Progress and Challenges," *Nanoscale Research Letters*, vol. 16, no. 1. Springer, 2021. doi: 10.1186/s11671-021-03628-6.

[15] R. N. Grimes, "Metallacarboranes in the new millennium," 2000. [Online]. Available: www.elsevier.com/locate/ccr

[16] N. Murphy, E. McCarthy, R. Dwyer, and P. Farràs, "Boron clusters as breast cancer therapeutics," *Journal of Inorganic Biochemistry*, vol. 218. Elsevier Inc., May 01, 2021. doi: 10.1016/j.jinorgbio.2021.111412.

[17] J. Olvera-Mancilla *et al.*, "Effect of metallacarborane salt H[COSANE] doping on the performance properties of polybenzimidazole membranes for high temperature PEMFCs," *Soft Matter*, vol. 16, no. 32, pp. 7624–7635, Aug. 2020, doi: 10.1039/d0sm00743a.

[18] M. Nuez-Martínez *et al.*, "Boron clusters (ferrabisdicarbollides) shaping the future as radiosensitizers for multimodal (chemo/radio/PBFR) therapy of glioblastoma," *J Mater Chem B*, vol. 10, no. 47, pp. 9794–9815, Oct. 2022, doi: 10.1039/d2tb01818g.

[19] D. E. Raeside, "Monte Carlo Principles and Applications," 1976.

[20] D. P. Kroese, T. Brereton, T. Taimre, and Z. I. Botev, "Why the Monte Carlo method is so important today," *Wiley Interdiscip Rev Comput Stat*, vol. 6, no. 6, pp. 386–392, Nov. 2014, doi: 10.1002/wics.1314.

[21] S. Agostinelli *et al.*, "GEANT4 - A simulation toolkit," *Nucl Instrum Methods Phys Res A*, vol. 506, no. 3, pp. 250–303, Jul. 2003, doi: 10.1016/S0168-9002(03)01368-8.

[22] J. Perl, J. Shin, J. Schümann, B. Faddegon, and H. Paganetti, "TOPAS: An innovative proton Monte Carlo platform for research and clinical applications," *Med Phys*, vol. 39, no. 11, pp. 6818–6837, 2012, doi: 10.1118/1.4758060.

[23] R. J. Van De Graaff, K. T. Compton, and L. C. Van Atta, "PHYSICAL REVIEW The Electrostatic Production of High Voltage for Nuclear Investigations," 1933.

[24] N. José and S. Catarino, "Campus Tecnológico e Nuclear Van de Graaff MANUAL DE OPERAÇÃO."

[25] A. Mazzone, P. Finocchiaro, S. Lo Meo, and N. Colonna, "On the (un)effectiveness of proton boron capture in proton therapy," *Eur Phys J Plus*, vol. 134, no. 7, Jul. 2019, doi: 10.1140/epjp/i2019-12725-8.

[26] T. Shtam *et al.*, "Experimental validation of proton boron capture therapy for glioma cells," *Sci Rep*, vol. 13, Mar. 2023, doi: 10.1038/s41598-023-28428-z.

A

APPENDIX A

```
25
26 s:So/MySource/Type                      = "Beam"
27 s:So/MySource/Component                 = "BeamPositio"
28 s:So/MySource/BeamParticle              = "proton"
29 d:So/MySource/BeamEnergy                = 1.975 MeV
30 u:So/MySource/BeamEnergySpread          = 0.0
31 s:So/MySource/BeamPositionDistribution  = "Gaussian"
32 s:So/MySource/BeamPositionCutoffShape   = "Ellipse"
33 d:So/MySource/BeamPositionCutoffX       = 1. um #X extentOfPosition
34 d:So/MySource/BeamPositionCutoffY       = 1. um #Y extentOfPosition
35 d:So/MySource/BeamPositionSpreadX       = 0.015 mm
36 d:So/MySource/BeamPositionSpreadY       = 0.015 mm
37 s:So/MySource/BeamAngularDistribution   = "Gaussian"
38 d:So/MySource/BeamAngularCutoffX        = 90. deg
39 d:So/MySource/BeamAngularCutoffY        = 90. deg
40 d:So/MySource/BeamAngularSpreadX        = 0.0002 rad
41 d:So/MySource/BeamAngularSpreadY        = 0.0002 rad
42 i:So/MySource/NumberOfHistoriesInRun    = 50000
```

TOPAS code 1 - Parametrization of the beam source

```
57 s:Ge/Cito/Type                = "TsSphere"
58 s:Ge/Cito/Parent              = "world"
59 s:Ge/Cito/Material            = "Water_75eV"
60 d:Ge/Cito/TransX              = 0 cm
61 d:Ge/Cito/TransY              = 0 cm
62 d:Ge/Cito/TransZ              = -5.4039 mm
63 d:Ge/Cito/RotX                = 0 deg
64 d:Ge/Cito/RotY                = 0 deg
65 d:Ge/Cito/RotZ                = 0 deg
66 d:Ge/Cito/RMin                = 0 um
67 d:Ge/Cito/RMax                = 15.0 um
68 d:Ge/Cito/SPhi                = 0 deg
69 d:Ge/Cito/DPhi                = 360 deg
70 d:Ge/Cito/STheta              = 0 deg
71 d:Ge/Cito/DTheta              = 180 deg
72 s:Ge/Cito/DrawingStyle        = "Solid"
73 s:Ge/Cito/Color               = "red"
74
```

TOPAS code 2 - Parametrization of the cytoplasm

```
75
76 s:Ge/Nuc/Type                = "TsSphere"
77 s:Ge/Nuc/Parent              = "Cito"
78 s:Ge/Nuc/Material            = "Boron"
79 d:Ge/Nuc/TransX               = 0 cm
80 d:Ge/Nuc/TransY               = 0 um
81 d:Ge/Nuc/TransZ               = 0 cm
82 d:Ge/Nuc/RotX                 = 0 deg
83 d:Ge/Nuc/RotY                 = 0 deg
84 d:Ge/Nuc/RotZ                 = 0 deg
85 d:Ge/Nuc/RMin                 = 0 mm
86 d:Ge/Nuc/RMax                 = 5 um
87 d:Ge/Nuc/SPhi                 = 0 deg
88 d:Ge/Nuc/DPhi                 = 360 deg
89 d:Ge/Nuc/STheta               = 0 deg
90 d:Ge/Nuc/DTheta               = 180 deg
91 s:Ge/Nuc/DrawingStyle         = "Solid"
92 s:Ge/Nuc/Color                = "blue"
93
94 sv:Ma/Boron/Components  = 1 "Boron"
95 uv:Ma/Boron/Fractions   = 1 1.0
96 d:Ma/Boron/Density      = 2.34 g/cm3
97
```

TOPAS code 3 - Parametrization of the nucleus made of boron with 10 µm diameter

```
138
139 s:Ge/Folha/Type     = "TsBox"
140 s:Ge/Folha/Material = "Mylar"
141 s:Ge/Folha/Parent   = "World"
142 d:Ge/Folha/HLX      = 6.35 mm
143 d:Ge/Folha/HLY      = 6.35 mm
144 d:Ge/Folha/HLZ      = 6.3 um
145 d:Ge/Folha/TransX   = 0. mm
146 d:Ge/Folha/TransY   = 0. mm
147 d:Ge/Folha/TransZ   = 5.9874 mm
148 d:Ge/Folha/RotX     = 0. deg
149 d:Ge/Folha/RotY     = 0. deg
150 d:Ge/Folha/RotZ     = 0. deg
151
152 s:Ge/FolhaFina/Type     = "TsBox"
153 s:Ge/FolhaFina/Material = "Mylar"
154 s:Ge/FolhaFina/Parent   = "World"
155 d:Ge/FolhaFina/HLX      = 6.35 mm
156 d:Ge/FolhaFina/HLY      = 6.35 mm
157 d:Ge/FolhaFina/HLZ      = 3.15 um
158 d:Ge/FolhaFina/TransX   = 0. mm
159 d:Ge/FolhaFina/TransY   = 0. mm
160 d:Ge/FolhaFina/TransZ   = 7.99685 mm
161 d:Ge/FolhaFina/RotX     = 0. deg
162 d:Ge/FolhaFina/RotY     = 0. deg
163 d:Ge/FolhaFina/RotZ     = 0. deg
164
```

TOPAS code 4 - Parametrization of the mylar layers

```
114 s:Sc/MyScore/Quantity                    = "DoseToMedium"
115 s:Sc/MyScore/Component                   = "Cito"
116 b:Sc/MyScore/OutputToConsole             = "TRUE"
117 s:Sc/MyScore/IfOutputFileAlreadyExists   = "Overwrite"
118 sv:Sc/MyScore/Report                     = 2 "Sum", "Mean"
119
120 s:Sc/MyScor/Quantity                   = "DoseToMedium"
121 s:Sc/MyScor/Component                  = "Nuc"
122 b:Sc/MyScor/OutputToConsole            = "TRUE"
123 s:Sc/MyScor/IfOutputFileAlreadyExists = "Overwrite"
124 sv:Sc/MyScor/Report                    = 2 "Sum", "Mean"
125
126 s:Sc/EnergyDep/Quantity                   = "EnergyDeposit"
127 s:Sc/EnergyDep/Component                  = "Cito"
128 b:Sc/EnergyDep/OutputToConsole            = "TRUE"
129 s:Sc/EnergyDep/IfOutputFileAlreadyExists = "Overwrite"
130 sv:Sc/EnergyDep/Report                    = 2 "Sum", "Mean"
131
132 s:Sc/EnergyDp/Quantity                   = "EnergyDeposit"
133 s:Sc/EnergyDp/Component                  = "Nuc"
134 b:Sc/EnergyDp/OutputToConsole            = "TRUE"
135 s:Sc/EnergyDp/IfOutputFileAlreadyExists = "Overwrite"
136 sv:Sc/EnergyDp/Report                    = 2 "Sum", "Mean"
```

TOPAS code 5 - Parametrization of the scorers of dose and energy deposition for the cytoplasm and nucleus

```
 95 s:Sc/EnergySpectrum/Quantity                    = "Fluence"
 96 s:Sc/EnergySpectrum/Component                   = "Cito"
 97 s:Sc/EnergySpectrum/IfOutputFileAlreadyExists   = "Overwrite"
 98 s:Sc/EnergySpectrum/OutputType                  = "CSV"
 99 sv:Sc/EnergySpectrum/OnlyIncludeParticlesNamed  = 1 "proton"
100 i:Sc/EnergySpectrum/EBins                       = 200
101 d:Sc/EnergySpectrum/EBinMin                     = 0 MeV
102 d:Sc/EnergySpectrum/EBinMax                     = 2 MeV
103
104 s:Sc/EnergySpectrumNuc/Quantity                 = "Fluence"
105 s:Sc/EnergySpectrumNuc/Component                = "Nuc"
106 s:Sc/EnergySpectrumNuc/IfOutputFileAlreadyExists = "Overwrite"
107 s:Sc/EnergySpectrumNuc/OutputType               = "CSV"
108 sv:Sc/EnergySpectrumNuc/OnlyIncludeParticlesNamed = 1 "proton"
109 i:Sc/EnergySpectrumNuc/EBins                    = 200
110 d:Sc/EnergySpectrumNuc/EBinMin                  = 0 MeV
111 d:Sc/EnergySpectrumNuc/EBinMax                  = 2 MeV
112
```

TOPAS code 6 - Parametrization of the energy spectrums for the cytoplasm and nucleus

```
 6 s:Sc/CountA/Quantity = "OriginCount"
 7 s:Sc/CountA/Component = "Cito"
 8 sv:Sc/CountA/OnlyIncludeParticlesNamed = 1 "alpha"
 9 b:Sc/CountA/OutputToConsole             = "TRUE"
10 s:Sc/CountA/IfOutputFileAlreadyExists = "Overwrite"
11
12 s:Sc/CountB/Quantity = "OriginCount"
13 s:Sc/CountB/Component = "Nuc"
14 sv:Sc/CountB/OnlyIncludeParticlesNamed = 1 "alpha"
15 b:Sc/CountB/OutputToConsole             = "TRUE"
16 s:Sc/CountB/IfOutputFileAlreadyExists = "Overwrite"
```

TOPAS code 7 - Parametrization of the origin count for alpha particles

B

APPENDIX B

Output 1 - Calculation of the number of protons for the first irradiation

SPE	Raw Q (nC)	Qf	Time (s)	Number of protons	Flux	Flux density (cm^{-2} s^{-1})
512005	22.75	2.48E-01	91	3.52E+10	3.87E+08	4.45E+09
512006	18	1.54E-01	72	1.74E+10	2.41E+08	2.77E+09
512007	30.25	1.24E-02	121	2.34E+09	1.94E+07	2.23E+08
512008	30.25	3.06E-02	121	5.77E+09	4.77E+07	5.49E+08
512009	30.25	6.16E-03	122	1.16E+09	9.53E+06	1.10E+08
512010	30.25	6.33E-03	121	1.19E+09	9.87E+06	1.14E+08
512011	71.5	5.30E-03	286	2.37E+09	8.27E+06	9.52E+07
512012	30.25	4.54E-03	121	8.57E+08	7.08E+06	8.15E+07
512013	30.25	5.59E-03	121	1.06E+09	8.72E+06	1.00E+08
512014	30.25	5.25E-03	122	9.91E+08	8.12E+06	9.34E+07
512015	30.25	4.91E-03	121	9.28E+08	7.67E+06	8.82E+07
512016	30.25	5.56E-03	121	1.05E+09	8.68E+06	9.98E+07
512017	30.25	9.35E-03	121	1.76E+09	1.46E+07	1.68E+08
			Average	1.26E+09	8.49E+06	1.05E+08
			sd	1.59E+09	1.39E+07	2.54E+07
			%	1.26E+00	1.64E+00	2.41E-01

Because of the instability of the beam, not all values were considered for the average. The values considered were the ones delimited by the red lines, meaning only the runs when the beam was more stable were considered.

SPE is the program gives to identify the run.

Output 2 - Calculation of the number of protons for the second irradiation

SPE	Charge (nC)	Time (s)	Number of protons	Flux
361038R1._	0.1065	61	6.65E+08	1.09E+07
361039R1._	0.0695	61	4.34E+08	7.11E+06
361040R1._	0.0474	61	2.96E+08	4.85E+06
361041R1._	0.0506	61	3.16E+08	5.18E+06
361042R1._	0.0442	61	2.76E+08	4.52E+06
361043R1._	0.0823	61	5.14E+08	8.42E+06
361044R1._	0.0804	61	5.02E+08	8.23E+06
361045R1._	0.0572	65	3.57E+08	5.49E+06
361046R1._	0.069	61	4.31E+08	7.06E+06
361047R1._	0.0606	61	3.78E+08	6.20E+06
361049R1._	0.1055	61	6.59E+08	1.08E+07
361066R1._	0.039	61	2.43E+08	3.99E+06
361067R1._	0.0394	61	2.46E+08	4.03E+06
		Average	4.09E+08	6.68E+06
		sd	1.43E+08	2.36E+06
		%	3.50E-01	3.53E-01

A

ANNEX A

A.1 Densities

Density of boron: $\rho_{boron} = 2.34\ g/cm^3$
Density of air: $\rho_{air} = 0.001225\ g/cm^3$
Density of mylar: $\rho_{mylar} = 1.38\ g/cm^3$
Density of water: $\rho_{water} = 1\ g/cm^3$

A.2 Definitions of flux, flux density and fluence

Flux – particles passing through an area per unit of time
Units in this works' context: [p s^{-1}]

Flux density – flux per unit of area
Units in this works' context: [p cm^{-2} s^{-1}]

Fluence – total amount of particles that went through a surface
Units in this works' context: [p cm^{-2}]